Table VI. Products of the Reactions of Lithium 2,3,3-Trimethylindolenide and Its 5-Methoxy Derivative with Methyl Chloride at 19 °C

5-substituent	solvent	concn, M	C/N	% reactn[a]
H	THF	0.27	4.9	46
			5.2	80
CH_3O	THF	0.25	13	50
			11	69
			8.3	72
H	dioxolane	0.50	9.3	58
			9.9	62
CH_3O	dioxolane	0.50	9.6	67
			12	77

[a] The reactions were terminated at these values, which therefore do not reflect absolute yields.

The ^{13}C chemical shift data for the 5-methoxy derivative are given in Table V. Because of the presence of the methoxy substituent, a direct comparison of the absolute chemical shifts of C(5) with those for the unsubstituted indolenide cannot be made. The changes in $\delta_{C(5)}$ from one solvent to another, however, are rather similar to those for the unsubstituted salt. The main difference is found in the temperature dependences (Figure 4) for the THF solutions. The changes in $\delta_{C(5)}$ in the lower end of the temperature range are a result of the conversion of monomer to dimer with increasing temperature, and this process begins at a much lower temperature in the case of the 5-methoxy derivative. This result is consistent with our findings in the lithium phenolate series in which conversion of dimers to tetramers occurs as the basicity of the phenolate ion is increased by appropriate para substitution. At the higher end of the temperature range, desolvation of the dimers is presumably also occurring, as has been observed for lithium *N*-isopropylanilide in THF.[11]

Methylation of Lithium Indolenides. The C- and N-methylation products of both indolenides have characteristic ^1H NMR spectra, which readily permit the total analysis of mixtures of starting material and products. Both gave essentially complete C-methylation when reacted with methyl iodide in either THF or dioxolane. In contrast, dimethyl sulfate yielded only the N-methylated products. Methyl chloride, however, gave mixtures of both C- and N-methylated derivatives and was selected for this preliminary study. Pyridine is too readily alkylated itself to be used as a solvent, and the 5-methoxyindolenide was too insoluble in diethyl ether for this solvent to be used. Accordingly, only reactions in THF and dioxolane were screened. The results are presented in Table VI. Although they are of a preliminary nature, they appear to indicate that aggregation does play a role in controlling the regiochemistry in the alkylation of lithium enamides, with C-methylation being favored by increased association.

Conclusions. The combination of observations of ^{13}C chemical shifts and ^6Li–^{15}N coupling constants, together with colligative measurements, used to study lithium arylamides also provides evidence for the solution structures of lithium enamides, which also appear to exist as either monomeric or dimeric ion pairs in weakly polar solvents.

A consideration of ^7Li quadrupole splitting constants leads to the conclusion that the lithium indolenide has the same π-bonded structure in solution in diethyl ether as found in the crystalline diethyl ether solvate. In the less sterically demanding solvent, dioxolane, the tetrasolvated dimer is formed.

A total of 4 equiv of HMPT appears to induce the same conversion to a triple-ion salt, $[LiA_2S_n]^-[Li(HMPT)_4]^+$, as found for lithium *N*-isopropylanilide.

Lithium 5-methoxy-2,3,3-trimethylindolenide also forms monomeric and dimeric ion pairs but with a greater propensity for the latter than the unsubstituted indolenide.

Methylation by methyl chloride gives both *C*- and *N*-methyl derivatives, the former being favored by the dimeric salts. These preliminary studies do not preclude the complex interplay of salt effects found in analogous reactions of lithium enolates.[12b]

The 2,3,3-trimethylindolenide system, with its fixed stereochemistry and variable regiochemistry, appears to be eminently suitable for a detailed mechanistic study of its alkylation.

Acknowledgment. We gratefully acknowledge support for this research by a grant (CHE85-03502) from the National Science Foundation (L.M.J.) and one (GM35982) from the National Institutes of Health (P.G.W.).

Registry No. HMPT, 680-31-9; $Li(HMPT)_4^+$, 56929-83-0; ^{15}N, 14390-96-6; ^6Li, 14258-72-1; Li^+, 17341-24-1; $C_{11}H_{12}NLi{\cdot}C_4H_{10}O$, 115560-36-6; 2,3,3-trimethylindolenine, 1640-39-7; 3,3-dimethyl-2-ethylindolenine, 18781-53-8; (4-methoxyphenyl)hydrazine, 3471-32-7; 2-methyl-3-pentanone, 565-69-5; 3,3-dimethyl-2-ethyl-5-methoxyindolenine, 115560-34-4; 1-methyl-2-methylene-2,3-dihydro-1*H*-indole, 115560-35-5; lithium 2,3,3-trimethylindolenide, 115590-27-7; lithium 5-methoxy-2,3,3-trimethylindolenide, 115603-36-6.

Thermodynamic Studies of Competitive Adduct Formation: Single- and Double-Insertion Reactions of Carbon Monoxide with Rhodium Octaethylporphyrin Dimer

Virginia L. Coffin, W. Brennen, and Bradford B. Wayland*

Contribution from the Department of Chemistry and the Laboratory for Research on the Structure of Matter, The University of Pennsylvania, Philadelphia, Pennsylvania 19104-6323.
Received November 4, 1987

Abstract: Reactions of carbon monoxide with (octaethylporphyrin)rhodium dimer, $[(OEP)Rh]_2$, in toluene produce an equilibrium system involving four species: $[(OEP)Rh]_2$ (**1**), $[(OEP)Rh]_2(CO)$ (**2**), (OEP)RhC(O)Rh(OEP) (**3**), and (OEP)RhC(O)C(O)Rh(OEP) (**4**). No evidence is found for the formation of a dicarbonyl adduct of **1**, which is accounted for on the basis of required structural features of metal–metal-bonded porphyrin dimers. ^1H and ^{13}C NMR evidence is presented for double insertion of CO into the Rh–Rh bond. NMR methods are used to determine enthalpy and entropy changes for the reaction of **1** with CO to form the following: **2**, $\Delta H_2° = -10 \pm 1$ kcal/mol (-41 ± 4 kJ/mol), $\Delta S_2° = -26 \pm 4$ cal/K·mol (-109 ± 17 J/K·mol); **3**, $\Delta H_3° = -12 \pm 2$ kcal/mol (-50 ± 8 kJ/mol), $\Delta S_3° = -31 \pm 5$ cal/K·mol (-130 ± 21 J/K·mol); **4**, $\Delta H_8° = -21 \pm 2$ kcal/mol (-88 ± 8 kJ/mol), $\Delta S_8° = -62 \pm 5$ cal/K·mol (-259 ± 30 J/K·mol). Thermodynamic criteria for the double insertion of CO into metal–metal bonds are presented and applied to the (OEP)Rh system.

Binding and activation of CO by transition-metal complexes has occupied a focal point in organometallic catalysis research. Reactions of coordinated CO with nucleophiles and CO insertions into M–R (R = alkyl, aryl) bonds are ubiquitous organometallic

0002-7863/88/1510-6063$01.50/0

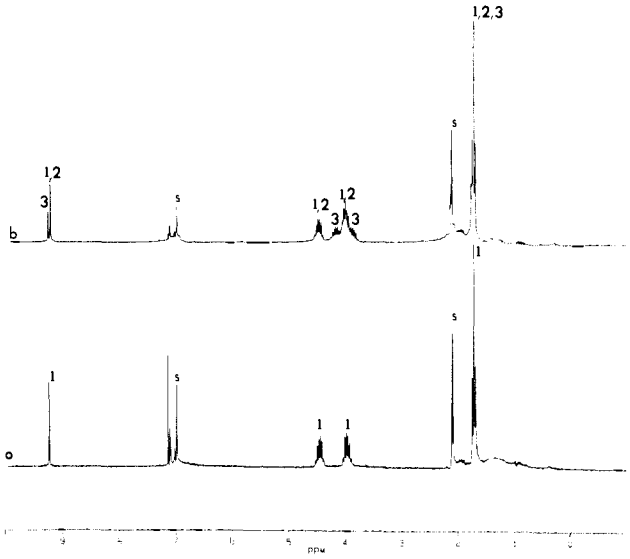

Figure 1. 250-MHz ^{1}H NMR at 298 K in toluene-d_8: (a) $[(OEP)Rh]_2$, (b) $[Rh(OEP)]_2$ + CO (P_{CO} = 603 ± 5 Torr). Compounds: **1**, $[(OEP)Rh]_2$; **2**, $[(OEP)Rh]_2(CO)$; **3**, (OEP)RhC(O)Rh(OEP).

processes that have been extensively studied.[1,2] Insertion of carbon monoxide into transition-metal–metal bonds[3-5] and MC(O)X units are quite rare,[6] and multiple insertions of CO into M–X bonds have not yet been reported.

We have previously reported that rhodium octaethylporphyrin dimer, $[(OEP)Rh]_2$ (**1**) reacts with CO at room temperature to produce an equilibrium distribution with two monocarbonyl complexes.[5] Terminal CO adduct formation gives a carbonyl adduct, $[(OEP)Rh]_2(CO)$ (**2**), while insertion of CO into the Rh–Rh bond gives a dirhodium ketone, (OEP)RhC(O)Rh(OEP) (**3**). Further studies of this system at lower temperatures and elevated pressures have revealed a third reaction corresponding to insertion of two CO molecules into the Rh–Rh bond to form $(OEP)RhC_2O_2Rh(OEP)$ (**4**), which is partially characterized by ^{1}H and ^{13}C NMR. This paper also reports thermodynamic parameters for reactions of **1** with CO to form **2–4** and an analysis of these values in terms of the Rh–C bond energies and standard bond energies for analogous organic compounds. The bond energies and observed entropy changes are used in the discussion of the thermodynamic criteria for observation of single and double insertion of CO into metal–metal bonds at equilibrium.

Results and Discussion

^{1}H NMR for toluene-d_8 solutions of $[(OEP)Rh]_2$ in the absence and presence of CO (P_{CO}^{298} = 0.793 ± 0.007 atm, T = 297 K)

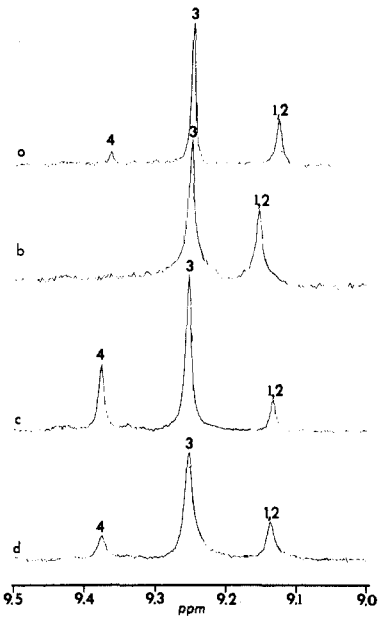

Figure 2. Methyne region of the 200-MHz ^{1}H NMR of $[Rh(OEP)]_2$ + CO in toluene-d_8 showing the effect of CO pressure and temperature: (a) P_{CO} = 20.6 atm, T = 297 K; (b) P_{CO} = 5.3 atm, T = 297 K; (c) P_{CO} = 20.6 atm, T = 260 K; (d) P_{CO} = 5.3 atm, T = 260 K. Compounds: **1**, $[(OEP)Rh]_2$; **2**, $[(OEP)Rh]_2(CO)$; **3**, (OEP)RhC(O)Rh(OEP); **4**, (OEP)RhC(O)C(O)Rh(OEP).

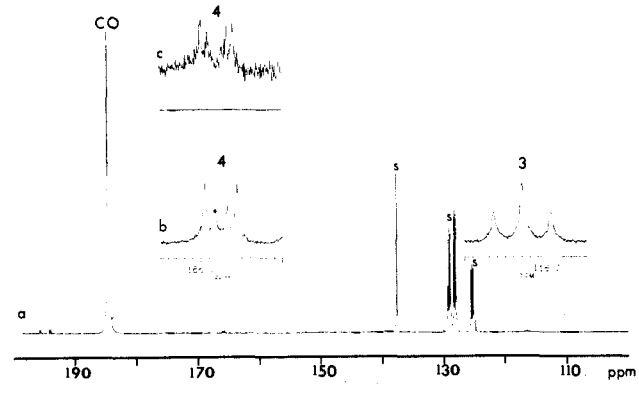

Figure 3. 125-MHz ^{13}C NMR of $[(OEP)Rh]_2$ + ^{13}CO in toluene-d_8: (a) P_{CO}^{298} = 25 ± 3 atm of 99.3% ^{13}CO at 250 K; (b) expansion of the AA′XX′ pattern due to (OEP)RhC(O)C(O)Rh(OEP) (**4**) at δ 165.7 and the triplet due to (OEP)RhC(O)Rh(OEP) (**3**) at δ 116.4; (c) P_{CO}^{298} = 22 ± 3 atm of 30% ^{13}CO at 250 K, expansion of the doublet of doublets due to (OEP)Rh^{13}C(O)^{12}C(O)Rh(OEP).

are illustrated in Figure 1. The singlet due to the porphyrin methyne hydrogens (δ 9.0–9.5) is sensitive to the substitution at rhodium and can be conveniently used to illustrate the changing distribution of (OEP)Rh species as a function of CO pressure and temperature. The methylene pattern (δ 3.5–4.5) is the AB portion of an ABX_3 pattern in which the magnetic inequivalence of H_a and H_b is highly sensitive to the proximity of the two porphyrin rings.

As the CO pressure and temperature are varied, reversible changes occur in the relative areas of the methyne peaks and the observed chemical shift of the highest field methyne peak (Figure 2). If the CO is removed by freeze–pump–thaw cycles, the sample reverts completely to $[(OEP)Rh]_2$ (**1**). We have interpreted these reversible changes in terms of three simultaneous equilibria involving **1**, CO, and three CO-containing (OEP)Rh complexes. One complex is in limiting fast exchange with **1** on the ^{1}H NMR time scale and is assigned to a terminal CO adduct, $[(OEP)Rh]_2(CO)$ (**2**). Two of the CO-containing complexes are in limiting slow exchange with **1** and ^{13}CO, and these species have been assigned to single and double CO insertion products, (OEP)RhC(O)Rh(OEP) (**3**) and $(OEP)RhC_2O_2Rh(OEP)$ (**4**).

(1) For instance, see: (a) Darensbourg, D. J.; Baldwin, B. J.; Froelich, J. A. *J. Am. Chem. Soc.* **1980**, *102*, 4688–4694. (b) Ungermann, C.; Landis, V.; Moya, S. A.; Cohen, H.; Walker, H.; Pearson, R. G.; Rinker, R. G.; Ford, P. C. *J. Am. Chem. Soc.* **1979**, *101*, 5922–5929. (c) Angelici, R. J. *Acc. Chem. Res.* **1972**, *5*, 335–341. (d) Gladyz, J. A. *Advances in Organometallic Chemistry*; Stone, F. G. A., West, R., Eds.; Academic: New York, 1982; Vol. 20, pp 1–38.

(2) (a) See: Alexander, J. J. In *The Chemistry of the Metal-Carbon Bond*, Hartley, F. R., Ed.; Wiley: New York, 1985; Vol. 2, Chapter 5, and references therein. (b) Berke, H.; Hoffmann, R. *J. Am. Chem. Soc.* **1978**, *100*, 7224–7236.

(3) (a) Colton, R.; McCormick, M. J.; Pannan, C. D. *Aust. J. Chem.* **1978**, *31*, 1425–1438. (b) Benner, L. S.; Balch, A. L. *J. Am. Chem. Soc.* **1978**, *100*, 6099–6106. (c) Kullberg, M. L.; Kubiak, C. P. *Inorg. Chem.* **1986**, *25*, 26–30. (d) Lee, C.; James, B. R.; Nelson, D. A.; Hallen, R. T. *Organometallics* **1984**, *3*, 1360–1364.

(4) (a) Brown, M. P.; Puddephatt, R. J.; Rashidi, M.; Manojlovic-Miur, Lj.; Muir, K. W.; Solomun, T.; Seddon, K. R. *Inorg. Chim. Acta* **1977**, *23*, L223–L224. (b) Brown, M. P.; Puddephatt, R. J.; Rashidi, M.; Seddon, K. R. *J. Chem. Soc., Dalton Trans.* **1978**, 1540–1544.

(5) Wayland, B. B.; Woods, B. A.; Coffin, V. L. *Organometallics* **1986**, *5*, 1059–1062.

(6) Sheridan, J. B.; Han, S. H.; Geoffroy, G. L. *J. Am. Chem. Soc.* **1987**, *109*, 8097–8098.

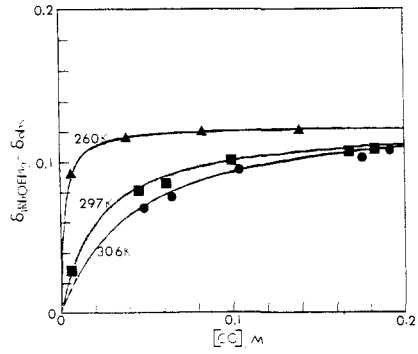

Figure 4. Dependence of the observed chemical shift of the methyne protons relative to the shift of the methyne protons in $[(OEP)Rh]_2$ as a function of CO concentration at three temperatures. The lines are calculated from the function: $\delta_1 - \delta_{obsd} = (\delta_1 - \delta_2)K_2[CO]/(1 + K_2[CO])$. Data for 260 K (▲), 297 K (■), and 306 K (●) are given. The fitted values are $\delta_1 - \delta_2 = 0.1225 \pm 0.005$ ppm, $K_2^{260} = 550 \pm 75$, $K_2^{298} = 48 \pm 4$, and $K_2^{306} = 25 \pm 2$. The values of K_c are referenced to unit activity at 1 M concentration for each component.

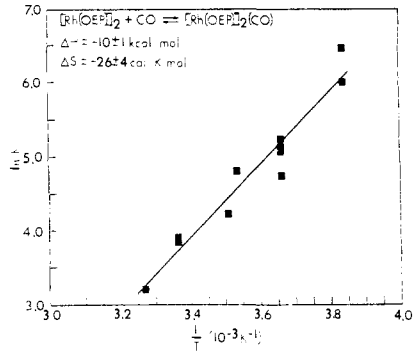

Figure 5. Van't Hoff plot for $[(OEP)Rh]_2 + CO \rightleftarrows [(OEP)Rh]_2(CO)$: ■, experimental points; —, calculated line.

The ^{13}C NMR of toluene-d_8 solutions of $[(OEP)Rh]_2$ with 99.3% ^{13}CO show a triplet at δ 116 ($J_{^{103}Rh-^{13}C}$ = 44 Hz) assigned to **3**, an AA'XX' multiplet at δ 165.5 assigned to **4**, and a broad resonance at δ 184 for ^{13}CO. The ^{13}C NMR spectrum for **2** is not observed due to exchange between free and coordinated ^{13}CO (Figure 3).

CO Adduct, $[(OEP)Rh]_2(CO)$. The chemical shift of the highest field methyne peak is dependent on temperature and CO pressure (Figure 2) and is ascribed to limiting fast exchange between equilibrium concentrations of **1** and **2** (reaction 1).[5] The observed

$$[(OEP)Rh]_2 + CO \rightleftarrows [(OEP)Rh]_2(CO) \qquad (1)$$

chemical shift, δ_{obsd}, of the highest field methyne peak is a weighted average of the chemical shift of the methyne hydrogens in **1** (δ_1) and **2** (δ_2). The pressure dependence (0.793 ± 0.007 atm $\leq P_{CO}^{298} \leq 22.6$ atm) of the observed chemical shift, relative to the shift in **1**, $\delta_1 - \delta_{obsd}$, has been fit to the equilibrium described by reaction 1 between 260 and 306 K to give the chemical shift difference between the methyne hydrogens in **1** and **2** ($\delta_1 - \delta_2$) and the equilibrium constant for adduct formation, K_1 (Figure 4). The calculated chemical shift difference, $\delta_1 - \delta_2$, is 0.1225 ± 0.005 ppm, and the ^1H NMR spectrum of **2** is assigned as δ 9.12 (s, C*H*), 4.45, 3.85 (m, CH_2CH_3), and 1.70 (t, CH_2CH_3). The assignment of **2** as a terminal CO adduct is supported by a CO stretching frequency of 2094 cm^{-1} in the IR of benzene solutions of $[(OEP)Rh]_2$ with CO ($P_{CO} \simeq 1$ atm).

The room-temperature molar equilibrium constant for CO adduct formation, K_1^{298}, is calculated to be 48 ± 4. The temperature dependence of K_1 over the range 260–306 K gives $\Delta H_1° = -10 \pm 1$ kcal/mol (-42 ± 4 kJ/mol); $\Delta S_1° = -26 \pm 4$ cal/K·mol (-109 ± 17 J/K·mol), and $\Delta G_1°(298\text{ K}) = -2.3 \pm 0.1$ kcal/mol (-9.6 ± 0.5 kJ/mol) (Figure 5). The limiting shift difference is observed for all of the samples ($P_{CO}^{298} \geq 0.793 \pm 0.007$ atm) below 245 K, indicating that coordination is essentially complete

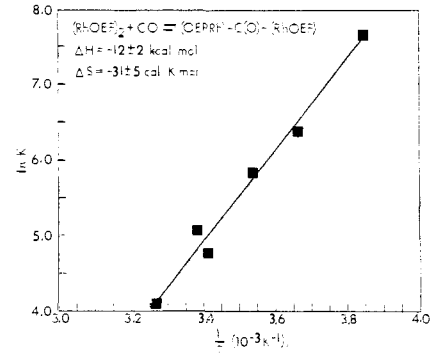

Figure 6. Van't Hoff plot for insertion of CO into $[(OEP)Rh]_2$: ■, experimental points; —, calculated line.

(>99%, **2**). No further temperature or CO pressure dependence of the shift could be detected down to 190 K, and we conclude that a dicarbonyl adduct does not contribute to the fast-exchange process.

$[(OEP)Rh]_2$ is a d^7–d^7 metal–metal single-bonded dimer with approximately square-pyramidal geometry about each metal atom where the second rhodium forms the apex of the square pyramid. Each Rh center contains a vacant coordination site, which could add CO to form a six-coordinate 18-electron Rh center. Carbon monoxide is observed to coordinate with one but not both Rh centers of $[(OEP)Rh]_2$.

The Rh–Rh bond energy in **1** has been measured as 16.5 ± 0.8 kcal/mol by NMR methods,[7] which is slightly smaller than the 18.7 ± 0.3 kcal/mol measured for $Rh_2(C_4H_8N_2O_2)_2(PPh_3)_2$[8] ($C_4H_8N_2O_2$ = dimethylglyoxime) by kinetic methods. The relatively weak Rh–Rh bond results from repulsive interactions between cofacial porphyrin rings, which restrict the mean interplanar spacing between the porphyrins to ~3.3 Å. To achieve the dimeric structure, the Rh atoms must be displaced out of the plane of the four nitrogens as seen for indium in (OEP)RhIn(OEP)[9] and in $[(OEP)Ru]_2$.[10] In the Ru–Ru double-bonded complex, $[(OEP)Ru]_2$, displacement of Ru from the donor atom plane is accompanied by significant doming of the porphyrin ligand in order to achieve the 2.408 Å Ru–Ru bond distance.

Addition of CO to a terminal site of $[(OEP)Rh]_2$ results in a competition between CO and the Rh–Rh bond for the same σ-bonding orbitals. We attribute the failure to observe a dicarbonyl adduct to an inability of **1** to form two effective Rh–CO bonds with retention of the Rh–Rh bond. Rh–Rh bond cleavage has been observed for $[(OEP)Rh]_2$ in the presence of excess donor molecules such as pyridine[11] and phosphites.[12] Cleavage of the Ru–Ru bond in $[(OEP)Ru]_2$ is also promoted by donor molecules.[13]

Single Insertion of CO, (OEP)RhC(O)Rh(OEP). The predominant CO-containing (OEP)Rh complex over the range of temperatures and pressures studied is shown to be a dirhodium ketone, (OEP)RhC(O)Rh(OEP) (**3**): ^1H NMR (toluene-d_8) δ 9.25 (s, C*H*), 4.18, 3.85 (m, CH_2CH_3), 1.70 (t, CH_2CH_3); IR (benzene solution) ν_{CO} = 1733 cm^{-1}; ^{13}C NMR $\delta_{C=O}$ 116 (t, $J_{^{103}Rh-^{13}C}$ = 44 Hz) (reaction 2).[5]

$$[Rh(OEP)_2] + CO \rightleftarrows (OEP)RhC(O)Rh(OEP) \qquad (2)$$

When solutions containing equilibrium concentrations of **3** are exposed to a fluorescent light source, **3** is selectively photolyzed

(7) Wayland, B. B.; Farnos, M.; Coffin, V. L. *Inorg. Chem.*, in press.
(8) Tinner, U.; Espensen, J. H. *J. Am. Chem. Soc.* **1981**, *103*, 2120–2121.
(9) Jones, N. L.; Carroll, P. J.; Wayland, B. B. *Organometallics* **1986**, *5*, 33–37.
(10) Collman, J. P.; Barnes, C. E.; Swepson, P. N.; Ibers, J. A. *J. Am. Chem. Soc.* **1984**, *106*, 3500–3510.
(11) Farnos, M. D. Ph.D. Dissertation, The University of Pennsylvania, 1986.
(12) Wayland, B. B.; Woods, B. A. *J. Chem. Soc., Chem. Commun.* **1981**, 475–476.
(13) Collman, J. P.; Brothers, P. J.; McElwee-White, L.; Rose, E.; Wright, L. J. *J. Am. Chem. Soc.* **1985**, *107*, 4570–4571.

Table I. Comparison of the ^1H NMR Spectra of Metal–Metal-Bonded, One-Atom-Bridged, and Two-Atom-Bridged Octaethylporphyrin Dimers[a]

	δ(-CH-)	$\delta(CH_aH_bCH_3)$	$\delta(CH_aH_bCH_3)$	$\delta(CH_2CH_3)$
$[Rh(OEP)]_2$	9.24 (s)	4.45 (m)	3.98 (m)	1.70 (t)
$[Ir(OEP)]_2$[b]	8.91 (s)	4.35 (m)	3.83 (m)	1.66 (t)
$[Mo(OEP)]_2$[b,15]	9.00 (s)	4.33 (m)	3.91 (m)	1.66 (t)
$[Rh(OEP)]_2(CO)$	9.12 (s)[d]	4.45 (m)	3.98 (m)	1.70 (t)
(OEP)RhC(O)Rh(OEP)	9.25 (s)	4.18 (m)	3.83 (m)	1.70 (t)
$(OEP)Rh(CO)_2Rh(OEP)$	9.38 (s)	3.99 (m)	3.74 (m)	1.72 (t)
$(OEP)Rh(CH_2)_2Rh(OEP)$	8.97 (s)	4.00 (m)	3.62 (m)	1.62 (t)
(OEP)RhCH=CHRh(OEP)[c]	8.94 (s)	3.76 (m)	3.68 (m)	1.71 (t)

[a] All spectra in toluene-d_8 referenced downfield from TMS except where noted. [b] Benzene-d_6. [c] THF-d_8. [d] Chemical shift is obtained by computer iteration.

Table II. Thermodynamic Values for the Reactions of Carbon Monoxide with $[(OEP)Rh]_2$

reaction	$\Delta H°$, kcal/mol (kJ/mol)	$\Delta S°$, cal/K·mol (J/K·mol)	$\Delta G_{298}°$, kcal/mol (kJ/mol)	K_c^{298}[a]
1	−10 ± 1 (−42 ± 4)	−26 ± 4 (−109 ± 17)	−2.3 ± 0.1 (−9.6 ± 0.4)	48 ± 4
2	−12 ± 2 (−50 ± 8)	−31 ± 5 (−130 ± 21)	−2.8 ± 0.1 (−11.7 ± 0.4)	125 ± 25
3	−2 ± 1 (−8 ± 4)	−5 ± 5 (−21 ± 21)	−0.5 ± 0.2 (−2.1 ± 0.8)	2.6 ± 0.5
8	−21 ± 2 (−88 ± 8)	−62 ± 5 (−259 ± 30)	−2.5 ± 0.1 (−10.5 ± 0.4)	64 ± 30
9	−9 ± 3 (−38 ± 13)	−31 ± 7 (−130 ± 29)	0.3 ± 0.3 (1.2 ± 1.2)	0.5 ± 0.2
10	−11 ± 1 (−46 ± 4)	−36 ± 3 (−151 ± 12)	−0.3 ± 0.1 (−1.2 ± 0.4)	1.4 ± 0.4

[a] The equilibrium constants, K_c, are referenced to the standard state with unit activity at 1 M concentration for each component.

to give **1**, **2**, and **4**. Due to the relatively slow formation of **3**, solutions were kept in the dark for 48 h prior to the NMR experiments and thermally equilibrated in the NMR spectrometer over a period of hours. Analysis of the areas of the methyne peaks due to **3** and **1** at known concentrations of CO gives the equilibrium constant, K_2, for reaction 2. The temperature dependence of K_2 gives enthalpy and entropy changes for reaction 2: $\Delta H_2° = -12 \pm 2$ kcal/mol (-50 ± 8 kJ/mol), $\Delta S_2° = -31 \pm 5$ cal/K·mol (-130 ± 21 J/K·mol), $\Delta G_2°(298\ K) = -2.8 \pm 0.1$ kcal/mol (-11.7 ± 0.4 kJ/mol), $K_2^{298} = 125 \pm 25$ (Figure 6).

The equilibrium constant, K_3, for the isomerization to form **3** from **2** (reaction 3) is a direct measure of the competition between

$$[(OEP)Rh]_2(CO) \rightleftarrows (OEP)RhC(O)Rh(OEP) \quad (3)$$

carbon monoxide adduct formation and insertion. The insertion product is favored by a ratio of 2.6/1 at 298 K ($K_3^{298} = 2.6 \pm 0.5$). A least-squares fit of ln K_3 vs $1/T$ gives $\Delta H_3° = -2 \pm 1$ kcal/mol (-8.4 ± 4 kJ/mol), $\Delta S_3° = -5 \pm 5$ cal/K·mol (-21 ± 21 J/K·mol), and $\Delta G_3°(298\ K) = -0.5 \pm 0.2$ kcal/mol (-2.1 ± 0.8 kJ/mol).

The enthalpy change for the general reaction of a metal–metal-bonded dimer with CO to form a dimetal ketone (reaction 4) can be expressed in terms of a set of bond energies (eq 5). The

$$M—M + CO \rightleftarrows M—C(O)—M \quad (4)$$

$$\Delta H_4° = (M—M) + (C{\equiv}O) - (C{=}O) - 2(M—C) \quad (5)$$

CO stretching frequencies for dimetal ketone complexes fall in the range 1638–1733 cm^{-1}, which suggests that the carbonyl unit in a dimetal ketone is similar to that in an organic ketone.[3-5] Using $[(C{\equiv}O) - (C{=}O)] = 70$ kcal/mol[14a] derived from thermochemical data on organic molecules results in the approximate relationship given by eq 6. For a reaction that combines two

$$-\Delta H_4° = 2(M-C) - (M-M) - 70\ \text{kcal/mol} \quad (6)$$

molecules to form one, an unfavorable entropy change of $\Delta S_4° = -30$ cal/K·mol ($-T\Delta S_4°(298\ K) \sim 9$ kcal/mol) is expected. A favorable free energy change, $\Delta G_4°(298\ K) < 0$, requires the metal–acyl carbon bond formed to exceed half the metal–metal bond broken by more than 39 kcal/mol, $[(M-C) - (M-M)/2] > 39$ kcal/mol (eq 7).

$$-\Delta G_4°(298\ K) \sim 2(M-C) - (M-M) - 79\ \text{kcal/mol} \quad (7)$$

Evaluating eq 6 for reaction 2 ($\Delta H_2° = -12 \pm 2$ kcal/mol; Rh–Rh = 16.5 ± 0.8 kcal/mol) gives an estimate of 49 ± 3 kcal/mol for the rhodium–acyl carbon bond energy in the dirhodium ketone, **3**. Formation of dimetal ketones from reaction of a metal–metal-bonded complex with CO is precedented for Pd(I)[3] and Pt(I)[4] "A-frame" complexes. Thermodynamic studies for the reactions of $Pd_2(dppm)_2(X)_2$ (X = Cl, Br, I, SCN)[3d] with CO in dimethylamine solvent yield enthalpy changes (-14.5 kcal/mol $\leq \Delta H \leq -11.5$ kcal/mol) that are similar to the value measured for reaction 2 ($\Delta H_2° = -12 \pm 2$ kcal/mol). If the metal–metal bonds are similar to or larger than in **1**, then the M–acyl carbon bonds in the A-frame complexes of Pd and Pt are comparable to or stronger than the Rh–acyl carbon bonds in **3**.

Double Insertion of CO, $(OEP)RhC_2O_2Rh(OEP)$. The third carbon monoxide containing (OEP)Rh complex, **4**, is observed by ^1H and ^{13}C NMR at high CO pressures ($P_{CO}^{298} > 12$ atm at 297 K) or at lower temperatures, where it is in limiting slow exchange with **1**, **2**, and ^{13}CO (Figure 2). The observed pressure dependence for the area of this methyne peak relative to the areas of the methyne peaks due to **2** and **3** indicates a ratio of 1/2 $[Rh(OEP)]_2/CO$ for compound **4**. The stoichiometry of the product is confirmed as 2/2 Rh(OEP)/CO by observation of an AA'XX' pattern in the ^{13}C NMR when **4** is formed by reaction of **1** with 99.3% ^{13}CO. The AA'XX' pattern requires two chemically equivalent but magnetically inequivalent ^{13}C and ^{103}Rh nuclei, which is compatible with a double-insertion product, (OEP)RhC(O)C(O)Rh(OEP), or a bis-adduct, (OC)[(OEP)-Rh]$_2$(CO). The CO adduct, $[(OEP)Rh]_2CO$, is in limiting fast exchange with **1** and CO by ^1H and ^{13}C NMR, and it is highly improbable that **4** could be a dicarbonyl adduct and be in the ^1H and ^{13}C NMR slow-exchange limit as observed for **4**.

Analysis of the area of the methyne peak due to **4** relative to those for **1–3** yields equilibrium constants for the double insertion

(14) (a) The value for $(C{\equiv}O) - (C{=}O)$ was obtained from $\Delta H°$ for the following reaction: R—R′(g) + CO(g) ⇄ R—C(O)—R′ $\Delta H = \Delta H_r°$; R = H, CH_3; R′ = H, CH_3. $\Delta H_r° = (R—R') + (C{\equiv}O) - (C{=}O) - (R—C(O)) - (R'—C(O))$. $[(C{\equiv}O) - (C{=}O)] = \Delta H_r° - (R—R') - (R—C(O)) - (R'—C(O))$. Standard bond energies[14c] were used for H–H (104 kcal/mol), CH_3–H (104 kcal/mol), CH_3–CH_3 (82 kcal/mol), H–C(O)R (87 kcal/mol), and H_3C–C(O)R (82 kcal/mol). $\Delta H_r°$ was calculated from the heats of formation of the reactants and products in the gas phase.[14c,d] (b) The $(C-C)_{diketone}$ bond energy is obtained from the following: $H_2(g) + 2CO(g) \rightleftarrows H—C(O)—C(O)—H$, $\Delta H° = +2.18$ kcal, $\Delta H° = (H—H) + 2[(C{\equiv}O) - (C{=}O)] - 2(H—C(O)) - (C-C)_{diketone}$ $(C-C)_{diketone} = 70$ kcal/mol, and $CH_3—C(O)—C(O)—CH_3 \rightarrow 2CH_3CO$, $\Delta H° = 69$ kcal, from the heats of formation of CH_3-C(O)-C(O)-CH_3[14c,d] and CH_3-C(O).[14e] (c) See: Cox, J. D.; Pilcher, G. *Thermochemistry of Organic and Organometallic Compounds*; Academic: New York, 1970. (d) Pedley, J. B.; Naylor, R. D.; Kibry, S. P. *Thermochemical Data of Organic Compounds*, 2nd ed.; Chapman and Hall: London, 1986. (e) Wagman, D. D.; Evans, W. H.; Parker, V. B.; Halow, I.; Bailey, S. M.; Schumm, R. H. NBS Technical Note 270-3; Institute for Basic Standards, National Burea of Standards: Washington, DC., 1968.

(15) Collman, J. P.; Barnes, C. E.; Woo, L. K. *Proc. Natl. Acad. Sci. U.S.A.* **1983**, *80*, 7684–7688.

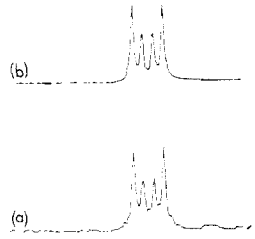

Figure 7. AA'XX' pattern in the ^{13}C NMR due to (OEP)RhC(O)C(O)Rh(OEP): (a) experimental spectrum at 125 MHz in toluene-d_8, P_{CO}^{298} = 25 ± 3 atm of 99.3% ^{13}CO at T = 250 K; (b) simulated spectrum with $^1J_{Rh-C}$ = 40 Hz, $^2J_{Rh-C}$ = 9 Hz, J_{Rh-Rh} = 4 Hz, and J_{C-C} = 20 Hz.

of CO into $[(OEP)Rh]_2$ (reaction 8) and for the reaction of CO with the mono-CO products to give **4** (reactions 9 and 10). Thermodynamic values for reactions 1–3 and 8–10 are summarized in Table II.

$$[(OEP)Rh]_2 + 2CO \rightleftarrows (OEP)RhC(O)C(O)Rh(OEP) \quad (8)$$

$$(OEP)RhC(O)Rh(OEP) + CO \rightleftarrows (OEP)RhC(O)C(O)Rh(OEP) \quad (9)$$

$$[(OEP)Rh]_2(CO) + CO \rightleftarrows (OEP)RhC(O)C(O)Rh(OEP) \quad (10)$$

Compound **4** occurs in an equilibrium distribution with **1–3** and becomes a prominent species only at relatively high CO pressures and lower temperatures. The necessity for high CO pressures, the low solubility of porphyrins, solvent absorptions, and overlapping bands in the ν_{CO} stretching region have thus far precluded a clear assignment of ν_{CO} for **4**. Inference of structural features for **4** is at present limited to ^1H and ^{13}C NMR where unambiguous assignments for compounds **1–4** can be made.

^1H NMR of the porphyrin hydrogens of several dimeric metallooctaethylporphyrin complexes are given in Table I. All of the known diamagnetic metal–metal-bonded metallooctaethylporphyrin dimers contain a widely split methylene pattern due to the magnetic anisotropy induced by the close proximity of the ring current from the two porphyrin rings. This feature is present in both **1** and **2** but not **4**. When the metal–metal bond is cleaved, the methylene pattern becomes less widely split, and the center of the pattern is shifted upfield. The methylene pattern for **4** shows the reduced splitting and upfield shift characteristic of two-atom-bridged complexes, markedly different from the metal–metal-bonded complexes. Both the limiting slow exchange of **4** with **1–3** and CO and the ^1H NMR of **4** clearly favor the double-insertion product over a dicarbonyl adduct.

The four observed lines of the AA'XX' pattern are not sufficient to give a unique solution for the four contributing coupling constants ($^1J_{^{103}Rh-^{13}C}$, $^2J_{^{103}Rh-^{13}C}$, $J_{^{103}Rh-^{103}Rh}$, and $J_{^{13}C-^{13}C}$). However, when **4** is formed by reaction of **1** with 30% ^{13}CO, the dominant product observed in the ^{13}C NMR is enriched at only one position (42% (OEP)Rh^{13}C(O)^{12}C(O)Rh(OEP)), giving rise to a doublet of doublets with $^1J_{^{103}Rh-^{13}C}$ = 40 Hz and $^2J_{^{103}Rh-^{13}C}$ = 9 Hz. When these values are fixed, the AA'XX' pattern may be simulated with J_{C-C} = ±20 Hz and J_{Rh-Rh} = ±4 Hz (Figure 7). A $^{13}C-^{13}C$ coupling constant of ~20 Hz provides clear evidence of C–C bond formation, but the value is smaller than those observed for organic diketones such as benzil ($J_{PhC(O)C(O)Ph}$ = 52 Hz).[16] Strained ketones such as cyclobutanone ($^1J_{^{13}C\pm^{13}C}$ = 21 Hz)[17] and complexes containing acetylene bonded perpendicular to a metal–metal bond ($^1J_{^{13}C-^{13}C}$ < 18 Hz)[18] are in the range observed in **4**. A one-bond $^{103}Rh-^{13}C$ coupling constant of 40 Hz is the range previously observed for (OEP)RhC(O)X complexes ((OEP)RhC(O)H, 29 Hz; (OEP)RhC(O)OCH$_2$CH$_3$, 46 Hz;[19] (OEP)RhC(O)Rh(OEP), 44 Hz) but substantially smaller than the 60–85 Hz reported for terminal CO complexes of rhodium.[20]

^1H and ^{13}C NMR clearly indicate that **4** results from inserting two CO units into the rhodium–rhodium bond of $[(OEP)Rh]_2$ to produce a rhodium–carbon-bonded bridging C_2O_2 fragment that contains a C–C bond. The similarity of the one-bond Rh–C coupling to other acyl complexes suggests that this fragment is best described as a 1,2-ethanedionyl bridge. Multicentered interactions between the (OEP)Rh and the C_2O_2 unit may account for the relatively small $^{13}C-^{13}C$ coupling constant (20 Hz) and relatively large two-bond $^{103}Rh-^{13}C$ coupling (9 Hz).

Formation of a 1,2-ethanedionyl bridging ligand by insertion and reductive coupling of CO (reaction 8) has not been previously observed, although it has been proposed as a carbon–carbon bond forming route in converting CO and H_2 to organic oxygenates.[21] Precedents for reductive coupling of CO are dominated by formation of ene–diolate and acetylene–diolate complexes, which are thermodynamically driven by strong M–O or Si–O bonding.[22-24] Studies of the decomposition of $(CO)_5MC(O)C(O)M(CO)_5$ (M = Mn, Re)[25] and the related $(CO)_5MnC(O)C(O)CH_3$[26] complexes formed by nucleophilic substitution indicate that negligible amounts of these complexes are present at equilibrium even in the presence of up to 100 atm of CO. In view of previous evidence against production of 1,2-ethanedionyl derivatives as thermodynamic products, we have analyzed the thermodynamic plausibility of insertion of two CO molecules into $[(OEP)Rh]_2$ (**1**) to form a bridging dionyl unit.

The enthalpy change for the general reaction of a metal–metal-bonded dimer with CO to form a bridged dionyl complex (reaction 11) can be expressed as a sum of bond energies (eq 12).

$$M—M + 2CO \rightleftarrows M—C(O)—C(O)—M \quad (11)$$

$$\Delta H_{12}^\circ \sim (M-M) + 2(C\equiv O) - 2(C=O) - 2(M-C) - (C-C)_{diketone} \quad (12)$$

Substitution of the terms $[(C\equiv O) - (C=O)]$ = 70 kcal/mol and $(C-C)_{diketone}$ = 70 kcal/mol[14] results in eq 13. The entropy loss

$$-\Delta H_{12}^\circ \sim 2(M-C) - (M-M) - 70 \text{ kcal/mol} \quad (13)$$

for combining three molecules to make one ($\Delta S^\circ \simeq -60$ cal/K·mol; $-T\Delta S^\circ(298\text{ K})$ = 18 kcal/mol) requires that the metal–acyl carbon bond energy exceed half the metal–metal bond energy by more than 44 kcal/mol ($[M-C) - (M-M)/2] > 44$ kcal/mol) in order to achieve a favorable free energy, $\Delta G^\circ(298\text{ K}) < 0$. Evaluating eq 13 for the Rh(OEP) system (reaction 8) with Rh–Rh = 16.5 ± 0.8 kcal/mol and ΔH_8° = −21 ± 3 kcal/mol gives an estimate of 54 ± 3 kcal/mol as the rhodium–acyl carbon bond energy in **4**.

(16) $J_{C(O)C(O)}$ = 51.8 Hz for benzil; $J_{C(N)C(N)}$ = 48.8 Hz for benzil hydrazone. Hansen, P. E.; Paulsen, O. K.; Berg, A. *Org. Magn. Reson.* **1975**, *7* 405.

(17) Wray, V. *Progress in Nuclear Magnetic Resonance Spectroscopy*; Emsley, J. W., Feeney, J.; Sutcliffe, L. H., Eds.; Pergamon: New York, 1980; Vol. 13, pp 177–256.

(18) Chisholm, M. H.; Folting, K.; Hoffman, D. M.; Huffman, J. C. *J. Am. Chem. Soc.* **1984**, *106*, 6794–6805 and references therein.

(19) Lissy, D. N. Ph.D. Dissertation, The University of Pennsylvania, 1986.

(20) Mann, B. E. *^{13}C NMR Data for Organometallic Compounds*; Academic: New York, 1981; Table 2.8.

(21) Daroda, R. J.; Blackborrow, J. R.; Wilkinson, G. *J. Chem. Soc., Chem. Commun.* **1980**, 1098–1099.

(22) (a) Manriquez, J. M.; McAllister, D. R.; Sanner, R. D.; Bercaw, J. E. *J. Am. Chem. Soc.* **1978**, *100*, 2716–2724. (b) Woczanski, P. T.; Bercaw, J. E. *Acc. Chem. Res.* **1980**, *13*, 121–127. (c) Berry, D. H.; Bercaw, J. E.; Jircitano, A. J.; Mertes, K. B. *J. Am. Chem. Soc.* **1982**, *104*, 4712–4715.

(23) (a) Fagan, P. J.; Manriquez, J. M.; Vollmer, S. H.; Day, C. S.; Day, V. W.; Marks, T. J. *J. Am. Chem. Soc.* **1981**, *103*, 2206–2220. (b) Fagan, P. J.; Moloy, K. G.; Marks, T. J. *J. Am. Chem. Soc.* **1981**, *103*, 6959–6962. (c) Moloy, K. G.; Fagan, P. J.; Manriquez, J. M.; Marks, T. J. *J. Am. Chem. Soc.* **1986**, *108*, 56–67. (d) Tatsumi, K.; Nakamura, A.; Hofmann, P.; Hoffmann, R.; Moloy, K. G.; Marks, T. J. *J. Am. Chem. Soc.* **1986**, *108*, 4467–4476.

(24) Bianconi, P. A.; Williams, I. D.; Engeler, M. P.; Lippard, S. J. *J. Am. Chem. Soc.* **1986**, *108*, 311–313. (b) Bianconi, P. A.; Vrtis, R. N.; Rao, C. P.; Williams, I. D.; Engeler, M. P.; Lippard, S. J. *Organometallics* **1987**, *6*, 1968–1977.

(25) de Boer, E. J. M.; de With, J.; Meijboom, N.; Orpen, A. G. *Organometallics* **1985**, *4*, 259–264.

(26) Casey, C. P.; Bunnell, C. A.; Calabrese, J. C. *J. Am. Chem. Soc.* **1976**, *98* 1166–1171.

For the specific case of Rh(OEP), the driving force for double insertion appears to be an increase in the rhodium–acyl carbon bond energy of ~5 kcal/mol upon insertion of the second CO.[27] An increase of this magnitude is plausible on steric grounds, since a Rh–C–Rh bond angle of at least 130° is necessary to accommodate the two porphyrin rings in **3**, whereas the bridging dionyl structure allows the porphyrin rings to be more nearly parallel, with a larger distance between the rings. The estimated rhodium–acyl carbon bond energies in **3** and **4** are slightly lower than the 58 kcal/mol obtained for the Rh–C bond in (OEP)RhC(O)H,[7] which establishes the thermodynamic plausibility for double insertion to occur in the Rh(OEP) system.

The more general reaction of CO insertion into a metal–acyl unit is depicted by eq 14. The dominant enthalpy changes in

$$MC(O)X + CO \rightleftarrows MC(O)C(O)X \qquad (14)$$

reaction 14 are associated with forming the C(O)–C(O) bond (–70 kcal/mol) and conversion of the CO triple bond to a double bond (+70 kcal/mol). Reaction 14 is expected to be thermodynamically unfavorable ($\Delta H_{14}° \sim 0$, $\Delta G_{14}°(298\ K) \sim +9$ kcal) unless the CO insertion is accompanied by an additional favorable energy term of at least 9 kcal mol^{-1}. Migratory insertion of CO into a M–acyl bond induced by reaction of the metal center with NO has recently been reported (eq 15).[6] This reaction uses the

$$Cp'(CO)_2MnC(O)tol + NO \rightleftarrows Cp'(CO)(NO)MnC(O)C(O)tol \qquad (15)$$

entrance of a new ligand to provide the favorable energy term to drive the CO insertion. The approximate thermodynamic criteria for reaction 14 imply that the Mn(NO) binding in the product must be at least 9 kcal stronger than the Mn(CO) binding in the reactant. The example of reaction 14 described in this paper has M = X = (OEP)Rh, and for this case we believe the additional favorable enthalpy term results from relief of steric strain that must be present in the dirhodium ketone, (OEP)RhC(O)Rh(OEP), and reduced in the double-insertion product.

Conclusions

A series of factors including a weak Rh–Rh bond, a strong Rh–C(O) bond, and the steric requirements of the porphyrin macrocycle have combined in the Rh(OEP) system to produce favorable thermodynamic factors for single and double insertion of CO into the Rh–Rh bond. At present, $[Rh(OEP)]_2$ is the only metal complex that reacts with CO to form a 1,2-ethanedionyl bridged complex, and thermodynamic considerations indicate that the unfavorable entropy change will prevent most systems from undergoing the second insertion, unless steric factors or coordination to oxygen provide additional favorable enthalpy terms.

Experimental Section

Synthesis of $[(OEP)Rh]_2$. (OEP)Rh(H) prepared by literature methods[28,29] is dissolved in 15–20 mL of degassed benzene and stirred for 1 week under vacuum with periodic freeze–pump–thaw cycles to remove evolved hydrogen. The benzene is stripped off on the vacuum line to yield $[(OEP)Rh]_2$.

Reagents. $[Rh(CO)_2Cl]_2$ and octaethylporphine ($OEPH_2$) were used as purchased from Aldrich. Grade 4.4 carbon monoxide from Air Products was run through Linde 3A molecular sieves at ambient temperature or a dry ice/acetone trap to remove water. ^{13}CO was used as purchased from MSD Isotopes (99.3 atom % ^{13}C). Toluene-d_8 from Aldrich was degassed by three freeze–pump–thaw cycles and then stored over Na/benzophenone or CaH_2.

Preparation of Samples for Thermodynamic Studies. Samples for thermodynamic measurements were prepared and sealed on a high vacuum line ($<10^{-4}$ Torr). The volume of the vacuum line was measured to ±1.5%. A total of 2–3 mg of $[(OEP)Rh]_2$ was placed in an NMR tube (o.d. 5 mm; i.d. 2.16 mm) sealed to a high-vacuum stopcock and evacuated overnight to remove residual water. Dried, degassed toluene-d_8 was distilled into the NMR tube from CaH_2 or Na/benzophenone. A measured amount of CO(g) was condensed into the NMR tube from the vacuum line at liquid-nitrogen temperature and the tube sealed.

The volume per unit length of the NMR tubes was measured by repeated weights with $CHCl_3$ (d = 1.787 g/mL at 20 °C) or Hg (d = 13.546 g/mL at 20 °C) to be 0.035 mL/cm. The CO was partitioned into the concentration of CO in solution, $[CO]_s$, and the pressure in the gas phase, P_{CO}^{298}, by iteration of eq 16.[30] P is the pressure in atmo-

$$[CO]_s = [4.405 \times 10^{-3} + 1.085 \times 10^{-5}(T_2)][P][T_1/T_2] \qquad (16)$$

spheres at T_1. T_1 is the laboratory temperature in Kelvin when the CO was condensed into the tube, and T_2 is set to 298 K to give $[CO]_s$ in moles per liter. For the samples used P_{CO}^{298} was 0.793 ± 0.007 (603 ± 5 Torr), 5.3 ± 2, 7.9 ± 2, 12.5 ± 2, 20.6 ± 2, and 22.6 ± 2 atm.

Variable-Temperature NMR. Variable-temperature ^1H NMR spectra were run on an IBM-Burker AF200SY or IBM-Bruker WP200SY spectrometer equipped with a Bruker VT-1000 temperature controller. The probe was cooled with an FTS systems refrigerator unit equipped with a temperature controller (220–283 K) or with the boil off from liquid nitrogen. Typical spectral parameters were OI = 2628 Hz, SW = 2994 Hz, and SI = 16 K. The digital resolution of the spectra (2SW/SI) was 0.365 Hz or 0.0018 ppm. Chemical shifts were referenced to the δ 2.09 residual proton peak of toluene-d_8 for a sample of $[(OEP)Rh]_2$ internally calibrated with a methanol capillary and the spectrometer reference maintained at that value for all spectra at that temperature. This sample also served as the temperature calibration for each set of measurements.[31]

Determination of the Equilibrium Constant for Adduct Formation. $[(OEP)Rh]_2$ (**1**) is in limiting fast exchange with $[(OEP)Rh]_2(CO)$ (**2**) in the ^1H NMR at all temperatures studied. For species in limiting fast exchange, the observed chemical shift of the methyne hydrogens, δ_{obsd}, is a weighted average of the chemical shift of the methyne hydrogens in $[(OEP)Rh]_2$, δ_1, and the methyne hydrogens in $[(OEP)Rh]_2(CO)$, δ_2 (eq 17). Substituting for χ_1 and rearranging gives eq 19 and the eq 20.

$$\delta_{obsd} = \delta_1\chi_1 + \delta_2\chi_2 \qquad (17)$$

$$\chi_1 + \chi_2 = 1 \qquad (18)$$

$$\delta_1 - \delta_{obsd} = (\delta_1 - \delta_2)\chi_2 \qquad (19)$$

$$\chi_2 = [[(OEP)Rh]_2(CO)]/\{[[(OEP)Rh]_2 + [(OEP)Rh]_2(CO)]\} \qquad (20)$$

Since the equilibrium constant for adduct formation is that given in eq 21, we can rearrange eq 21 and substitute into eq 20 to obtain eq 22. δ_1

$$K_2 = [[(OEP)Rh]_2(CO)]/[[(OEP)Rh]_2][CO] \qquad (21)$$

$$\delta_1 - \delta_{obsd} = (\delta_1 - \delta_1)K_2[CO]/(1 + K_2[CO]) \qquad (22)$$

$- \delta_{obsd}$ is obtained from the spectra. The concentration of CO is known for each sample from eq 16, using $T_2 = T$, T_1 = 298 K, and P_{CO}^{298}. The chemical shift of the methyne protons in **1** and the residual proton spectrum of toluene-d_8 are both temperature dependent, making the chemical shift difference ($\delta_1 - \delta_2$) the best parameter for comparison of data at different temperatures. The equilibrium constant, K_2, and the chemical shift difference between $[(OEP)Rh]_2$ and $[(OEP)Rh]_2(CO)$ ($\delta_1 - \delta_2$) are obtained by iteritive nonlinear least-squares curve fitting[32] of at least five samples at each temperature. The mean chemical shift

(27) The bond energy calculations used here are approximations, and the steric strain in the dirhodium ketone, **3**, would be expected to affect the C=O bond energy as well as the Rh–C bond energy, so that both of these bond energies contribute to the 9 kcal/mol increase in enthalpy for formation of the dionyl-bridged complex.

(28) (a) Setsuni, J.; Yoshia, Z.; Ogoshi, H. *J. Chem. Soc., Perkin Trans. 1* **1982**, 983–987. (b) Ogoshi, H.; Setsune, J.; Omura, T.; Yoshida, Z. *J. Am. Chem. Soc.* **1975**, *97*, 6461–6466.

(29) Abeysekera, A. M.; Grigg, R.; Trocha-Grimshaw, J.; Viswanatha, V. *J. Chem. Soc., Perkin Trans. 1* **1977**, 36–44, 1395–1403.

(30) This formula is a combination of the solubility of CO at 1 atm as a function of temperature, the density of toluene as a function of temperature and pressure, and the ideal gas law. (a) Gjaldbaek, J. *Acta Chem. Scand.* **1952**, *6*, 623. (b) Field, L. R.; Wilhelm, E.; Battino, R. *J. Chem. Thermodyn.* **1974**, *6*, 237. (c) Brunel, R. F.; Van Bibber, K. *Int. Crit. Tables 3*, 27. (d) Decombe, L.; Decome, J. *Int. Crit. Tables 3*, 38.

(31) The chemical shift difference between the hydroxyl protons and the methyl protons, $\Delta\nu$, is strongly temperature dependent for methanol. Over the temperature range 220–313 K, T (K) = 406.0 – 0.551($|\Delta\nu|$) – 63.4($\Delta\nu/100$)^2 at 60 MHz. At 306 K, the calibration was done with an external ethylene glycol sample for which the separation of the hydroxyl protons and the methylene protons as a function of temperature is T (K) = 466.4 – 1.705$|\Delta\nu|$ at 60 MHz for the range 297–415 K. See: Van Gleet, A. L. *Abstracts of Papers*, 10th Experimental NMR Conference; Mellon Institute: Pittsburgh, PA, March 1969.

(32) This was done on an IBM PC computer using a modified version of the simplex program in: Noggle, J. H. *Chemistry on a Microcomputer*; Little, Brown: Boston, 1985.

difference was determined to be 0.1225 ± 0.005 ppm for the temperature range 260–306 K.

In order to obtain shift data at temperatures below 260 K where the inserted products dominate, the samples were exposed to a fluorescent light source for 4–18 h at 297 K to photolyze (OEP)RhC(O)Rh(OEP) (**3**) and give predominantly **1** and **2**. The sample was then quenched to low temperature (190–273 K) in the NMR spectrometer and the spectrum recorded after 30 min.

Determination of the Equilibrium Constants for the CO-Insertion Reactions. The equilibrium distribution of **1**–**4** was obtained for three samples (P_{CO}^{298} = 5.3, 12.5, and 20.6 atm). The samples were kept away from light for at least 24 h prior to the experiment and during the experiment. NMR spectra were obtained at 30-min to 2-h intervals until three consecutive spectra showed no further changes in the relative areas of the peaks.

The concentration of each species was obtained as a fraction of the total concentration of all four species from the area of the methyne peaks, with the area of the peak due to the exchange partitioned into concentrations of **1** and **2** (eq 23–26). The equilibrium constants for reactions

$$[\mathbf{1}] = A_{1,2}/(A_{1,2} + A_3 + A_4)(1 + K_2[CO]) \quad (23)$$

$$[\mathbf{2}] = (A_{1,2})(K_2[CO])/(A_{1,2} + A_3 + A_4)(1 + K_2[CO]) \quad (24)$$

$$[\mathbf{3}] = A_3/(A_{1,2} + A_3 + A_4) \quad (25)$$

$$[\mathbf{4}] = A_4/(A_{1,2} + A_3 + A_4) \quad (26)$$

3–7 (vide supra) can then be calculated as in eq 27–31.

$$K_3 = [\mathbf{3}]/[\mathbf{1}][CO] \quad (27)$$

$$K_4 = [\mathbf{3}]/[\mathbf{2}] \quad (28)$$

$$K_5 = [\mathbf{4}]/[\mathbf{1}][CO]^2 \quad (29)$$

$$K_6 = [\mathbf{4}]/[\mathbf{3}][CO] \quad (30)$$

$$K_7 = [\mathbf{4}]/[\mathbf{2}][CO] \quad (31)$$

Enthalpy and entropy changes for reactions 1–3 and 8–10 were obtained from a least-squares fit of ln K vs $1/T$.

^{13}C NMR. ^{13}CO-enriched samples were prepared by the same procedure as described for the thermodynamic measurements but with 10-mm heavy-walled tubes for the samples at more than 1 atm of pressure. ^{13}CO was condensed from 1-L break-seal bulb, and the pressure for these samples is known to ±3 atm. The 30% ^{13}CO was obtained by mixing known volumes of natural-abundance CO and 99.3% ^{13}CO to obtain the reduced enrichment.

^{13}C NMR spectra were obtained on IBM-Bruker WP200SY, Bruker Instruments AF500SY, and Bruker Instruments WP360 spectrometers. The frequencies for carbon are 50.33, 125, and 96 MHz, respectively. Samples used contained 1 atm of 99.3% ^{13}CO, 25 atm of 99.3% ^{13}CO, and 22 atm of 30% ^{13}CO. NMR spectra were internally referenced to toluene-d_8 with the singlet at δ 137.5 downfield from TMS.

There is no change in the relative peak positions for the pattern at δ 165.5 (250 K) with temperature (220, 250, 273, and 297 K), spectrometer frequency (50.33, 96, and 125 MHz), or ^{1}H decoupling. The observed frequencies are at +24.5 ± 0.5, +8 ± 0.5, −8 ± 0.5, and −24.5 ± 0.5 Hz. When the enrichment is reduced to 30% ^{13}CO, the peak positions alter to become +24.5 ± 1, +15.5 ± 1, −15.5 ± 1, and −24.5 ± 1 Hz. Simulation of the AA′XX′ patern was done on an IBM-Bruker W-P200SY spectrometer equipped with an Aspect 2000 computer by using the PANIC84 program supplied with the software.

(OEP)RhC(O)C(O)Rh(OEP), (OEP)RhC(O)Rh(OEP), and (OEP)RhC(O)H all exhibit temperature-dependent ^{13}C shifts for the carbonyl carbon, with the resonance shifting to high field by ~0.01 ppm K^{-1} for (OEP)RhC(O)C(O)Rh(OEP) and (OEP)RhC(O)H and by ~0.02 ppm K^{-1} for (OEP)RhC(O)Rh(OEP). Chemical shifts of acyl carbons in organic aldehydes and ketones have been observed to be temperature dependent, but the origin of the dependence is not fully understood.[33] The direction of the ^{13}C shifts of the inserted products away from ^{13}CO at δ 184 with increasing temperature and the similarity to (OEP)RhC(O)H argue against the temperature-dependent shifts being attributable to an exchange process involving ^{13}CO.

Acknowledgment. Support of this work by the Department of Energy, Division of Chemical Sciences, Office of Basic Energy Sciences, is gratefully acknowledged.

Registry No. 1, 63439-10-1; **2**, 101403-89-8; **3**, 101403-90-1; **4**, 115512-15-7; CO, 630-08-0.

(33) Anet, F. A. L. In *Topics in Carbon-13 NMR Spectroscopy*; Levy, G. C., Ed.; Wiley: New York, 1979; Vol. 3, p 79.